**Revista de Metalurgia**
October–December 2020, 56 (4), e183
ISSN-L: 0034-8570
https://doi.org/10.3989/revmetalm.183

# Formation and thermodynamic analyses of inclusions in Ti-containing steel weld metals with different Al contents

BingXin Wang[a,✉], XiangHua Liu[b], GuoDong Wang[b]

[a]College of Mechanical Engineering, Liaoning Shihua University, Fushun 113001, China
[b]State Key Laboratory of Rolling & Automation, Northeastern University, Shenyang 110004, China
(✉Corresponding author: wangbingxin@163.com)

Submitted: 24 April 2019; Accepted: 20 October 2020; Available On-line: 12 January 2021

**ABSTRACT:** The Ti-containing steel weld metals with Al contents of 0.01-0.085% were prepared. The effects of Al contents in weld metals on the inclusions evolution were in detail investigated by means of thermodynamic calculations coupled with electron probe micro-analyses. The results show that the inclusions in the 0.01% Al weld metal are mainly composed of ilmenite with more amounts of (Mn-Si-Al)-oxide and titanial-spinel. When Al content is increased up to 0.035%, a more amount of corundum and a small amount of pseudobrookite are formed. In 0.085% Al weld metal, the (Mn-Si-Al)-oxide phase disappears completely, and the inclusions contain a substantial amount of corundum, in addition to a minimal amount of pseudobrookite. $Ti_3O_5$, $MnTi_2O_4$ and $MnTiO_3$ are the primary constituents of pseudobrookite, titanial_spinel and ilmenite solid solutions, respectively. Titanial_spinel and ilmenite have higher amounts of Mn, but lower Ti levels compared with pseudobrookite.

**KEYWORDS:** Aluminium content; Electron probe micro-analyzer; Oxide inclusion; Phase diagram; Thermodynamic calculation; Weld metal

**Citation/Citar como:** Wang, B.X.; Liu, X.H.; Wang, D.G. (2020). "Formation and thermodynamic analyses of inclusions in Ti-containing steel weld metals with different Al contents". *Rev. Metal.* 56(4): e183. https://doi.org/10.3989/revmetalm.183

**RESUMEN:** *Formación y análisis termodinámico de inclusiones en metales de soldadura de acero que contienen Ti con diferentes contenidos de Al*. Se prepararon muestras de metales de soldadura de acero que contienen Ti con contenidos de Al de 0,01-0,085%. Los efectos del contenido de Al en los metales de soldadura sobre la evolución de las inclusiones se investigaron en detalle mediante cálculos termodinámicos junto con microanálisis de sonda de electrones. Los resultados muestran que las inclusiones en el 0,01% de metal de soldadura de Al están compuestas principalmente de ilmenita con más cantidades de (Mn-Si-Al) -óxido y titanial-spinel. Cuando el contenido de Al aumenta hasta un 0,035%, se forma una mayor cantidad de corindón y una pequeña cantidad de pseudobrookita. En el 0,085% de metal de soldadura de Al. En el metal de soldadura de 0,085% Al, la fase de óxido (Mn-Si-Al) desaparece por completo y las inclusiones contienen una cantidad sustancial de corindón, además de una cantidad mínima de pseudobrookita. $Ti_3O_5$, $MnTi_2O_4$ y $MnTiO_3$ son los componentes principales de las soluciones sólidas de pseudobrookita, titanial_spinel e ilmenita, respectivamente. Titanial-spinel e ilmenita tienen cantidades más altas de Mn, pero niveles más bajos de Ti en comparación con la pseudobrookita.

**PALABRAS CLAVE:** Cálculo termodinámico; Contenido de aluminio; Diagrama de fases; Inclusión de óxido; Metal de soldadura; Microanalizador de sonda de electrones

**ORCID ID:** BingXin Wang (https://orcid.org/0000-0002-3506-507X); XiangHua Liu (https://orcid.org/0000-0003-2870-175X); GuoDong Wang (https://orcid.org/0000-0002-9458-4638)

## 1. INTRODUCTION

It is well known that some fine non-metallic inclusions in weld metals and/or steels can strongly contribute to the nucleation of acicular ferrite (AF) (Lin *et al.*, 2018; Zhang *et al.*, 2018a), which can noticeably improve the toughness. Among the non-metallic inclusions, such as oxides, titanium nitride, vanadium nitride and manganese sulfide, Ti-containing oxide inclusions have been often reported to have strong ability to induce AF formation. Yamada *et al.* (2009) and Takada *et al.* (2015) pointed out that the TiO contributes to the nucleation of AF and that the AF nucleated on TiO shows the Baker-Nutting (B-N) orientation relationship with the TiO. This orientation relationship achieves good lattice coherency and decreases the interfacial energy between the AF and TiO, resulting in a decrease in activation energy for AF nucleation. Several researchers (Shim *et al.*, 2001; Kang and Lee, 2010; Seo *et al.*, 2015) have reported that a Mn-depleted zone (MDZ) can be detected around $Ti_2O_3$ inclusions in steels and weld metals, so that the local depletion of Mn around the inclusions promotes AF nucleation by increasing the chemical driving force. Shim *et al.* (1999) also proved the above results in a steel-$Ti_2O_3$ diffusion bonding experiment.

However, in the case of chemical compositions of commercial steels and/or ordinary weld metals, the complex Ti-containing oxide inclusions, such as $MnTi_2O_4$ and $MnTiO_3$, rather than simple ones mentioned above are usually formed (Kang *et al.*, 2016; Wang *et al.*, 2018). Therefore, it is much more meaningful to investigate the potency of complex Ti-containing oxide inclusions to nucleate the intragranular AF. Some researchers have done related investigations. Nako *et al.* (2014) and Kang *et al.* (2016) found that $MnTi_2O_4$ on the surfaces of the inclusions is responsible for the formation of AF. In their studies, it was revealed that AF can have not only the B-N orientation relationship with $MnTi_2O_4$ but also the Kurdjumov-Sachs (K-S) orientation relationship with the austenite matrix. Kang *et al.* (2016) reported that in the presence of large amounts of $MnTi_2O_4$ and $MnTiO_3$ constituents of inclusions, the Mn in the matrix around the inclusions is consumed, and as a result, the MDZ is developed.

Therefore, the formation of Ti-containing inclusions mentioned above is essential for AF nucleation regardless of Mn depletion or crystallographic lattice match mechanisms, and accurate control of the formation of such inclusions is very important. The chemical compositions of steels and/or weld metals have strong effect on the formation, types and structures of inclusions. Kang *et al.* (2014) studied the evolution of Ti-containing inclusions, and pointed that with an increase in the Ti content, the Ti-rich oxide is changed from $MnTi_2O_4$-rich spinel to the mixture of $Ti_2O_3$ and $MnTiO_3$, and the $Ti_2O_3$ content is increased. Moreover, some researchers also investigated the influences of Zr (Zou *et al.*, 2018), Mg (Zhang *et al.*, 2016) elements, etc., on the inclusions formation. As a strong deoxidizer, Al is usually used to deoxidize the liquid Fe solusion above the liquidus temperature of the liquid steel. Therefore, the steels and/or weld metals for structural applications inevitably contain a certain amount of Al element. Al should be expected to influence the oxide formation process in weld metals. However, so far few studies have been done to investigate the effect of Al element on the evolution of the inclusions in Ti-containing weld metals.

On the other hand, the formation of inclusions is rather complex because the inclusions found in ordinary weld metals and/or commercial steels usually consist of a mixture of several complex crystalline solid solutions and/or amorphous phases instead of simple stoichiometric compounds such as $Mn_2TiO_4$, $MnTi_2O_4$, $MnTiO_3$ and $Ti_2O_3$ (Kang *et al.*, 2016; Wang *et al.*, 2018). Therefore, it is a little difficult to accurately analyse the types, contents and of chemical compositions of constituent phases in inclusions only by means of experimental ways. By the commercial thermochemical computing package FactSage$^{TM}$, thermodynamic calculation approach can be used to effectively predict the formation of multi-phase inclusions based on the Gibbs free energy minimization principle. The FactSage commercial thermochemical computing package is very helpful in understanding the inclusions evolution, and has been widely applied to evaluate various complex non-metallic inclusion systems (Zhang *et al.*, 2018b; Li *et al.*, 2018).

The present study analysed how Al element affects the inclusions evolution including the types, contents and of chemical compositions of constituent phases of inclusions in Ti-containing steel weld metals using FactSage commercial thermochemical computing package combined with electron probe micro-analyzer.

## 2. MATERIALS AND METHODS

### 2.1. Weld metals preparation

Figure 1 indicates the process of weld metals preparation. Build-up welding using pure Fe powder was first performed in a 15 mm deep trapezoid slot in C-Mn steel plates with thickness of 20 mm, and then a V-groove with depth of 7 mm is again machined at the build-up welds. After that, a single pass submerged-arc welding (SAW) process is performed using a C-Mn steel welding wire with a diameter of 4 mm under a voltage of 35 V and current of 450 A. Three weld metals with different Al contents, but almost the same Ti and Mn concentrations were obtained by adding different amounts of pure Al powder and a certain amounts of Ti-Fe

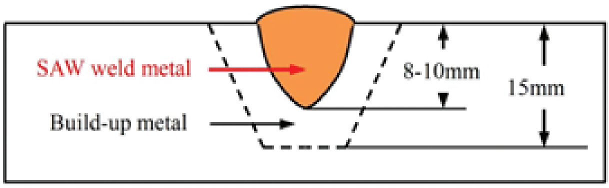


FIGURE 1. Schematic drawing showing the preparation of the weld metal.

TABLE 1. Chemical compositions of welding wire (mass, %)

| C | Mn | Si | S | P | Al |
|---|---|---|---|---|---|
| 0.05 | 0.86 | 0.06 | 0.022 | 0.02 | 0.01 |

powder (33% Ti) and Mn-Fe powder (81% Mn) to the groove prior to SAW. The chemical compositions of the welding wire and weld metals are listed in Table 1 and Table 2, respectively. In light of the Al content, weld metals were labeled as WL (0.01% Al), WM (0.035% Al) and WH (0.085% Al).

### 2.2. Inclusion analyses and thermochemical computing on the formation of inclusion

The specimens were cut from the weld metals, and examination planes perpendicular to the welding direction were prepared by mechanical polishing. The morphology and chemical compositions of the inclusions were analysed by a JEOL JXA-8530F electron probe micro-analyzer (EPMA).

The commercial thermochemical computing package FactSage$^{TM}$ (version 7.2) was employed to calculate the thermodynamic stability of various inclusion phases using the FToxid, FTmisc and FSstel databases containing model parameters, the thermodynamic properties and structures of thermodynamic models of the inclusion phases as functions of temperature and composition. According to the chemical compositions of weld metals and selected databases, the major constituent phases of inclusion considered in the present thermochemical calculations are as followed:

Pseudobrookite: $Ti_3O_5$-$FeTi_2O_5$-$MnTi_2O_5$ solid solution
Titanial_Spinel: (Mn, Fe)(Ti, Al)$_2$O$_4$ solid solution
Ilmenite: $Ti_2O_3$-$FeTiO_3$-$MnTiO_3$ solid solution
Corundum: $Al_2O_3$ + ($Ti_2O_3$ in dilute amount)
Stoichiometric compounds: all relevant stoichiometric compounds
Slag phase: $Al_2O_3$-$SiO_2$-MnO-$Ti_2O_3$-$TiO_2$-FeO multi-component liquid oxides solution formed by oxidation reactions of several elements in weld metals

The equilibrium cooling mode was applied to predict the formation of inclusions between 1000-1600 °C. Moreover, various reactions during further cooling in the solid state, were not considered, for simplicity.

Phase Diagram module was used to generate a ternary isothermal phase diagram at 1000 °C for the system containing $Al_2O_3$-MnO-$SiO_2$ components in order to study the effect of Al on the formation of complex inclusions.

## 3. RESULTS AND DISCUSSION

Figures 2-4 present the EPMA analysis results of inclusions in the weld metals containing different levels of Al. According to the chemical composition characteristics displayed in EPMA maps of the inclusions, the inclusion in WL is mainly composed of the (Mn-Si-Al)-oxide and (Mn-Ti)-oxide accompanied by a certain amount of Al-containing oxide phase and small amount of discrete MnS patches distributed at the periphery of the inclusion. Compared with the inclusion in WL, the amounts of (Mn-Ti)-oxide and Al-containing oxide of the inclusion in WM are increased, and (Mn-Si-Al)-oxide nearly disappears. In WH, as shown from EPMA maps, the Mn and Si element contents in the inclusion are lower than those of the matrix located near the inclusion. Due to the absence of Mn and Si, the inclusion predominantly consists of Al-oxide in addition to minimal amount of Ti-oxide, and does not contain (Mn-Si-Al)-oxide.

Figure 5 presents the thermodynamic analyses about inclusions evolution. It can be clearly observed from the constituent phases of the inclusions at 1000 °C (liquid oxides have been completely decomposed at this temperature) that, in WL, the inclusion contains a large amount of ilmenite solid solution in addition to more amounts of $Mn_2Al_4Si_5O_{18}$ and titanial_spinel. In WM, a large amount of corundum and a small amount of pseudobrookite are formed. Moreover,

TABLE 2. Chemical compositions of weld metals (mass, %)

| C | Mn | Si | S | P | Al | O | N | Ti |
|---|---|---|---|---|---|---|---|---|
| 0.050 | 3.01 | 0.203 | 0.014 | 0.029 | 0.010 | 0.040 | 0.0037 | 0.018 |
| 0.045 | 3.14 | 0.220 | 0.016 | 0.025 | 0.035 | 0.039 | 0.0041 | 0.020 |
| 0.056 | 2.98 | 0.271 | 0.014 | 0.026 | 0.085 | 0.037 | 0.0039 | 0.018 |

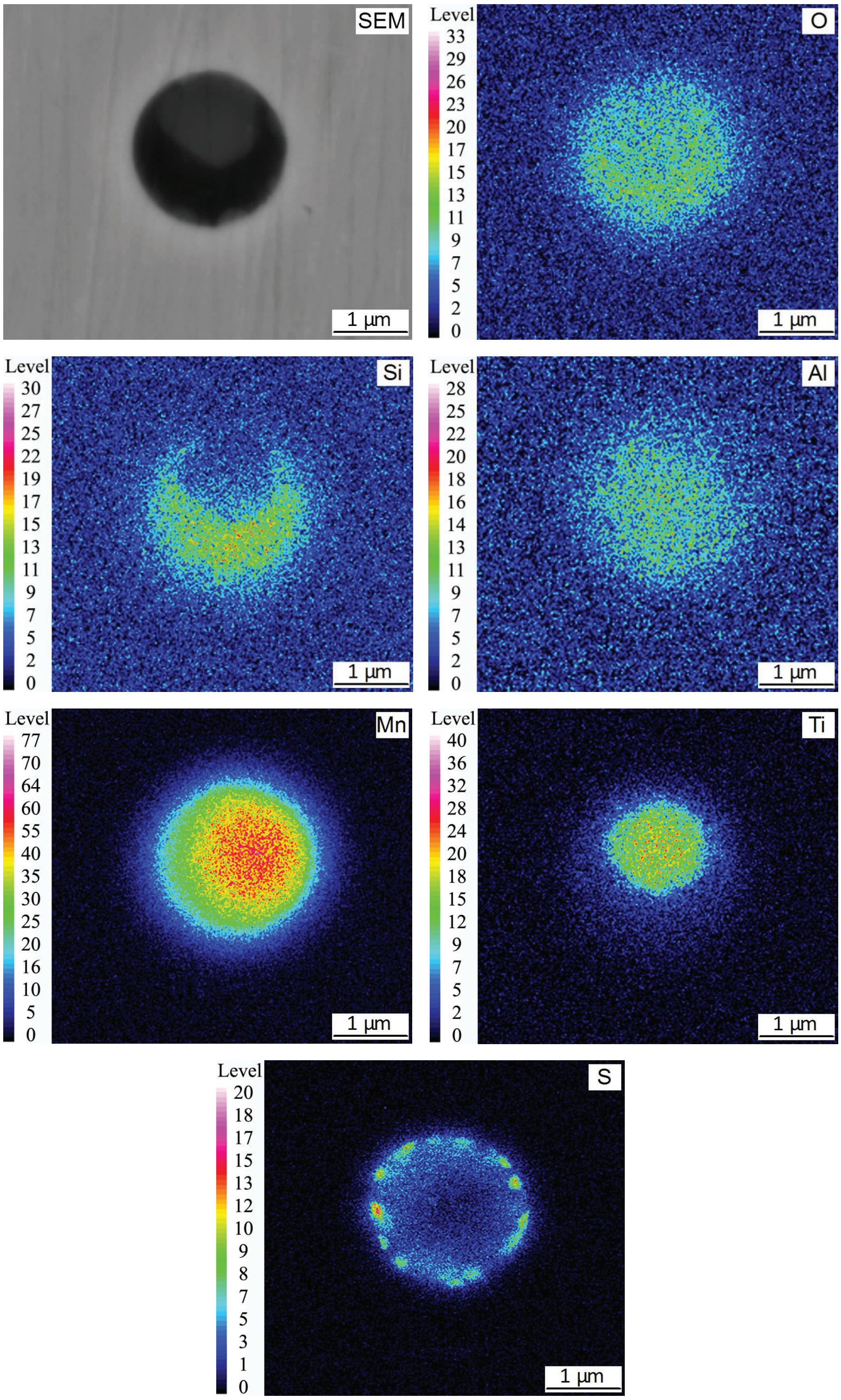


FIGURE 2. SEM image and EPMA maps of the inclusion in WL.

titanial_spinel solid solution and $Mn_2Al_4Si_5O_{18}$ compound disappear. In WH, the inclusion is mainly composed of corundum with minimal amount of pseudobrookite.

The constituent contents and chemical compositions of solid solution in the inclusions were obtained based on the thermodynamic calculation results, and shown in Fig. 6. $MnTi_2O_4$, $MnTiO_3$,

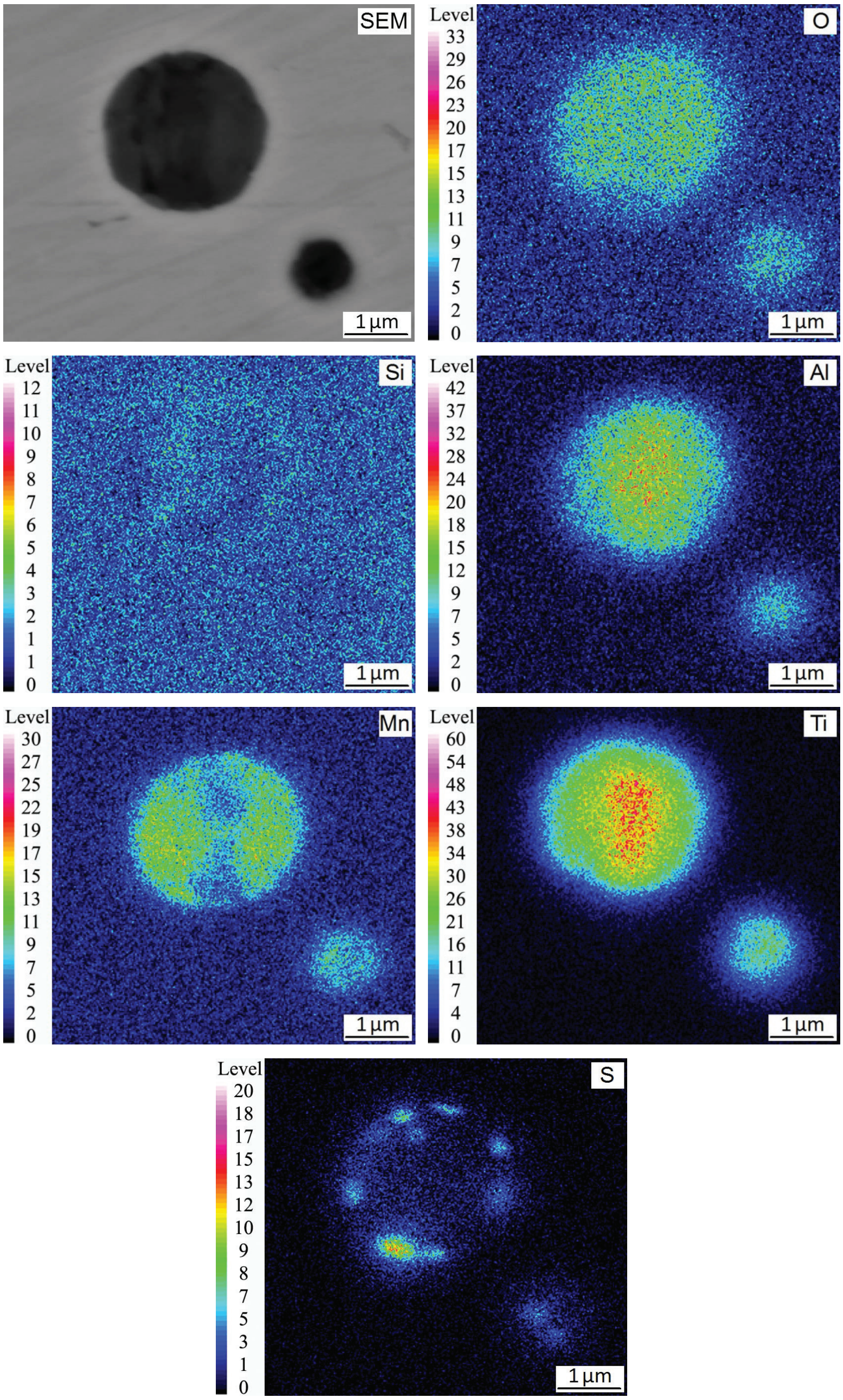


FIGURE 3. SEM image and EPMA maps of the inclusion in WM.

$Ti_3O_5$ and $Al_2O_3$ are the primary constituents in respective solid solutions (i.e., titanial_spinel, ilmenite, pseudobrookite and corundum). It is worth noting that although titanial_spinel, ilmenite and pseudobrookite are all Ti-rich solid solutions, titanial_spinel and ilmenite have higher amounts of Mn, but lower Ti levels compared with pseudobrookite.

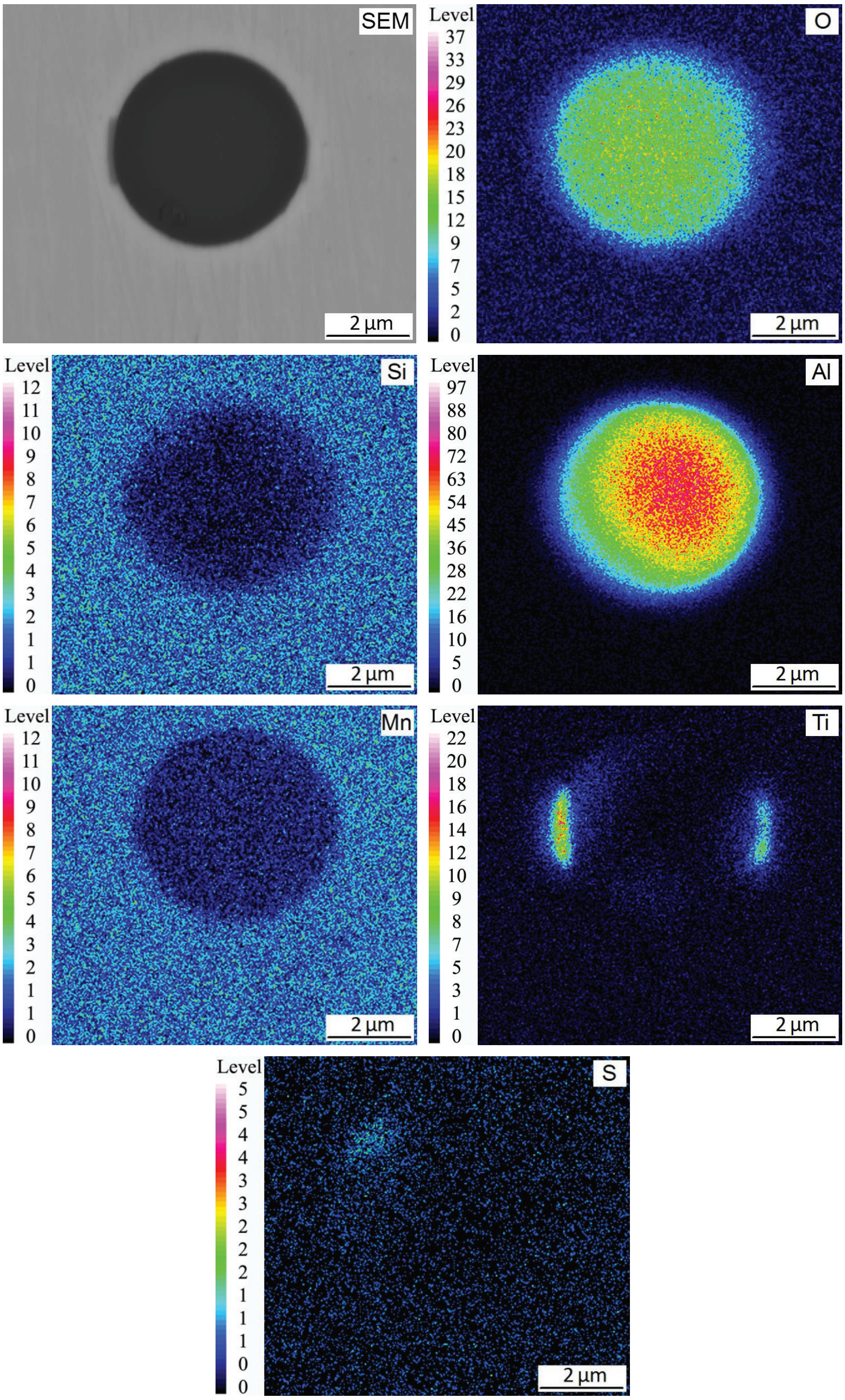


FIGURE 4. SEM image and EPMA maps of the inclusion in WH.

Based on thermodynamic calculations shown in Figs. 5, 6, it is clear that (Mn-Si-Al)-oxide appeared in EPMA analyses should be $Mn_2Al_4Si_5O_{18}$ compound, while Ti-containing phases are undoubtedly titanial_spinel, ilmenite and pseudobrookite solid solutions. Additionally, Al-containing oxide phase in EPMA maps should be corundum and titanial_spinel. Comparisons between Figs. 2-4 and Figs. 5, 6

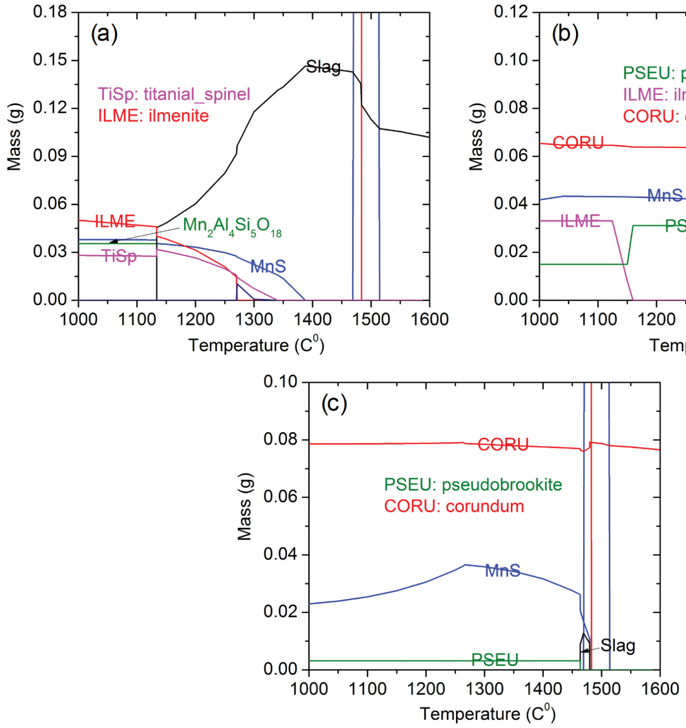

FIGURE 5. Thermodynamic analyses on inclusions evolution for (a) WL, (b) WM and (c) WH.

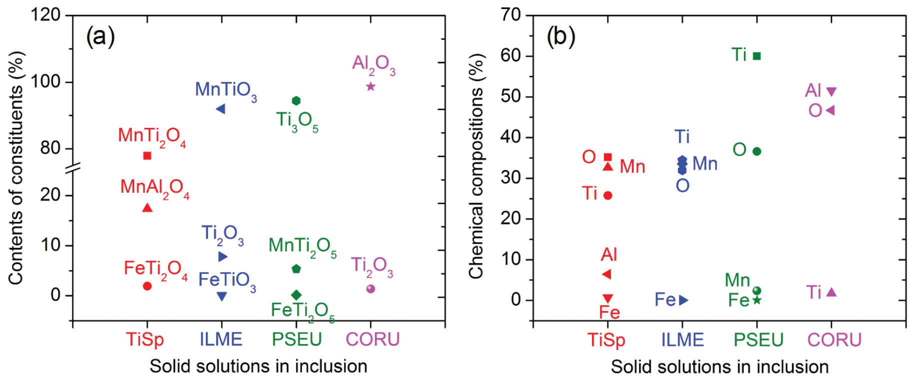

FIGURE 6. Constituent contents (a) and chemical compositions (b) of solid solutions.

show that thermodynamic analyses on constituents and chemical compositions characteristics of inclusions well agree with experimental results of EPMA maps.

As mentioned above, Al element has a strong effect on the formation and evolution of inclusions in weld metals. It is well known that during welding, a series of complex metallurgical physics chemical reactions are expected to take place in weld pool. Elements of Al, Ti, Si, Mn, etc., can combine with soluble oxygen in weld pool, which results in the formation of a variety of liquid oxides such as $Al_2O_3$, $TiO_x$ and MnO (i.e., molten slag) above liquidus temperature of slag, and the decrease in the amount of the dissolved oxygen in the weld pool. There are the competition relationships between Al, Ti, Si and Mn during oxidation process. Compared with Si and Mn elements, Al and Ti have much stronger affinities with oxygen under the same contents due to their lower oxygen potentials of forming oxides (Mitsutaka and Kimihisa, 2010). Moreover, the content of metal elements also has a noticeable effect on the oxidation process of metals. In order to clarify the effect of Al element content on the oxidation products, equilibrium calculation on compositions of liquid oxides at 1600 °C was carried out with Fe-0.05C-3.1Mn-0.23Si-0.014S-0.019Ti-0.039O-$x$Al ($0<x<0.09$) alloy system (in mass%) similar to the chemical compositions of weld metals, and shown in Fig. 7. Under low Al content (for example,

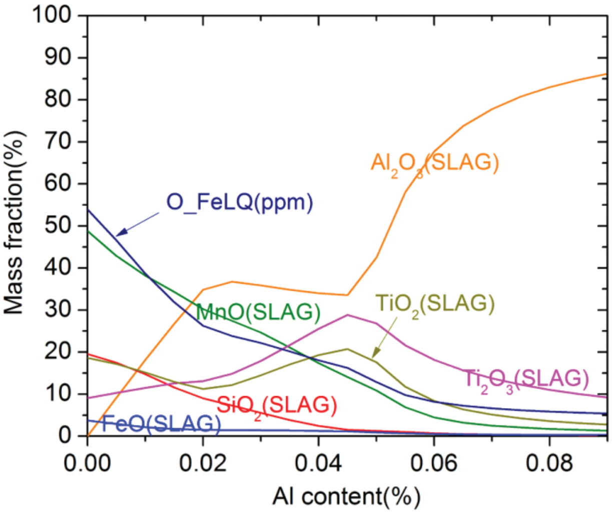


FIGURE 7. The variations in compositions of liquid oxides solutions with Al content at 1600 °C. O_FeLQ (in ppm) represents dissolved oxygen content in liquid Fe solution at 1600 °C.

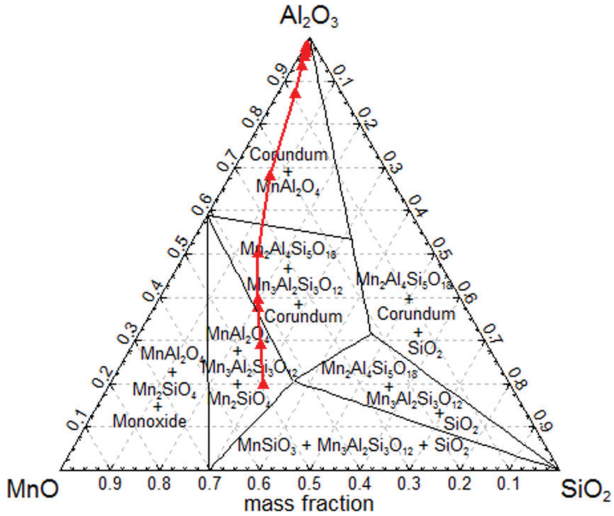


FIGURE 8. Ternary isothermal phase diagram of $Al_2O_3$-MnO-$SiO_2$ system at 1000 °C Red solid line with symbol is calculated inclusion trajectory using Equilib with Fe-3.1Mn-0.23Si-0.039O-*x* Al (0.01<*x*<0.09) alloy system (in mass%).

0.01% Al), despite high affinity with oxygen of Al, the amount of $Al_2O_3$ in oxidation product is lower compared with that of MnO due to high content of Mn element. With an increase in Al content, the amount of $Al_2O_3$ is strongly raised accompanied by the drops of other constituents such as MnO, $SiO_2$ and $TiO_2$. However, when content of Al is increased to the range of about 0.02-0.045%, the content of $Al_2O_3$ in liquid oxide is slightly lowered, while those of $Ti_2O_3$ and $TiO_2$ are increased. The combining ability with oxygen for metals dissolved in Fe solution (i.e., oxygen potential of forming corresponding oxides) is determined as followed (Mitsutaka and Kimihisa, 2010):

$$\pi_{O(M_xO_y)} = \Delta_r G_m^{\ominus} + \frac{2}{y} RT\ln a_{(M_xO_y)} - \frac{2x}{y} RT\ln a_{[M]} \quad (1)$$

where $a_{(MxOy)}$ and $a_{[M]}$denote the activities of $M_xO_y$ in the liquid oxide solution and the metal element dissolved in liquid Fe solution, respectively.

The liquid oxide and liquid Fe solutions can be regarded as ideal solutions. Thus, the concentrations (mole ratio) of $M_xO_y$ in the liquid oxide solution and the metal element dissolved in liquid Fe solution are respectively their activities (Mitsutaka and Kimihisa, 2010).

When the Al content is increased up to a certain range (for example, 0.02-0.045%), the liquid oxide solution can contain higher amount of $Al_2O_3$, which increases the activity of $Al_2O_3$, but lowers the activities of other constituents including $TiO_x$ (i.e., $Ti_2O_3$ and $TiO_2$) in liquid oxide solution. Therefore, according to Eq. (1), the oxygen potentials of forming $TiO_x$ oxides should be lowered, which can promote the formation of $TiO_x$. Meanwhile, the amount of $Al_2O_3$ can be lowered due to the competition relationship between Al and Ti. When the content of Al is further increased (for example, more than 0.045%), according to Eq. (1), the oxygen potential of forming $Al_2O_3$ can be lowered. Thus, a large amount of $Al_2O_3$ can form to strongly consume soluble oxygen in liquid Fe solution. The decrease of soluble oxygen in liquid Fe solutions is expected to suppress the oxidation reactions of other metal elements including Ti (Hsieh *et al.*, 1996), which leads to a remarkable decrease in the amounts of $TiO_x$, MnO, $SiO_2$ and so on, so that the amounts of MnO and $SiO_2$ are very low in the case of very high Al content, for example 0.085%.

During cooling after welding, different kinds and amounts of constituent phases in inclusions are expected to precipitate in light of the chemical compositions characteristics of liquid oxides. In order to further demonstrate this effect, slag compositions in equilibrium at 1600 °C were calculated with Fe-3.1Mn-0.23Si-0.039O-*x*Al (0.01<*x*<0.09) alloy system (in mass%), and superimposed to a ternary isothermal diagram of $Al_2O_3$-MnO-$SiO_2$ system at 1000 °C to reveal the inclusion path with Al content, as shown in Fig. 8. Al_spinel (mainly $MnAl_2O_4$) and olivine (mainly $Mn_2SiO_4$) do not appear in the case of present compositions in weld metals, as shown in Fig.5. Thus, with the increase of $Al_2O_3$ amount (correspondingly, the contents of MnO and $SiO_2$ are lowered), the evolution of Al-containing oxide phases is followed as: $Mn_3Al_2Si_3O_{12}$→corundum+ $Mn_3Al_2Si_3O_{12}$+ $Mn_2Al_4Si_5O_{18}$ →corundum.

In the case of 0.01% Al, the liquid oxide contains a large amount of MnO constituent and a certain amounts of $TiO_x$, which favours the formations of titanial_spinel and ilmenite rather than pseudobrookite. Similarily, the formation of (Mn-Si-Al)-oxide is also promoted due to high amount of MnO and a certain amount of $SiO_2$, as shown in Fig. 2. When Al level is increased up to 0.035%, as analysed above, the amounts of $Ti_2O_3$, $TiO_2$ and $Al_2O_3$ constituents in molten slag are increased, but those of MnO and $SiO_2$ are correspondingly decreased, which results in formations of pseudobrookite and corundum at the expense of amount of (Mn-Si-Al)-oxide in the inclusions, as shown in Fig. 3. In the case of 0.085% Al, the liquid oxide is mainly composed of $Al_2O_3$ with small amounts of $TiO_x$. Meanwhile, the amounts of $SiO_2$ and MnO in the liquid oxide are very low, and in particular, the $SiO_2$ content is almost zero, resulting in the absence of (Mn-Si-Al)-oxide in the inclusions. Similarly, a very low content of MnO accompanied by small amounts of $TiO_x$ contributes to the formation of a small amount of pseudobrookite. Thus, the inclusions have a very high amount of corundum and a very low content of pseudobrookite, as shown in Fig. 4.

## 4. CONCLUSIONS

- The kinds and amounts of the constituent phases of the inclusions are remarkably changed with the Al content in the weld metals. The inclusions in the 0.01% Al weld metal are mainly composed of ilmenite with more amounts of (Mn-Si-Al)-oxide and titanial_spinel. When Al content is increased up to 0.035%, a more amount of corundum and a small amount of pseudobrookite are formed. In 0.085% Al weld metal, the (Mn-Si-Al)-oxide phase disappears completely, and the inclusions contain a substantial amount of corundum, in addition to a minimal amount of pseudobrookite.
- $Ti_3O_5$, $MnTi_2O_4$ and $MnTiO_3$ are the primary constituents of pseudobrookite, titanial_spinel and ilmenite solid solutions, respectively. Titanial_spinel and ilmenite have higher amounts of Mn, but lower Ti levels compared with pseudobrookite.

## ACKNOWLEDGMENTS

This work was financially supported by a Project of Education Department of Liaoning Province (grant no. L2016132). Authors are grateful to Drs. H.Y. Wu, W.N. Zhang (State Key Laboratory of Rolling & Automation of Northeastern University, China), and L.Z. Kong (School of Metallurgy of Northeastern University, China) for providing helps in EPMA analyses works and thermodynamic calculations.

## REFERENCES

Hsieh, K.C., Babu, S.S., Vitek, J.M., David, S.A. (1996). Calculation of inclusion formation in low-alloy-steel welds. *Mater. Sci. Eng. A* 215 (1-2), 84-91. https://doi.org/10.1016/0921-5093(96)10370-1.

Kang, Y.B., Lee, H.G. (2010). Thermodynamic analysis of Mn-depleted zone near Ti oxide inclusions for intragranular nucleation of ferrite in steel. *ISIJ Int*. 50 (4), 501-508.

Kang, Y.J., Jang, J.H., Park, J.H., Lee, C.H. (2014). Influence of Ti on non-metallic inclusion formation and acicular ferrite nucleation in high-strength low-alloy steel weld metals. *Met. Mater. Int.* 20 (1), 119-127. https://doi.org/10.1007/s12540-014-1013-1.

Kang, Y.J., Jeong, S.H., Kang, J.H., Lee, C.H. (2016). Factors affecting the inclusion potency for acicular ferrite nucleation in high-strength steel welds. *Metall. Mater. Trans. A* 47, 2842-2854. https://doi.org/10.1007/s11661-016-3456-0.

Li, J.Y., Cheng, G.G., Ruan, Q., Pan, J.X., Chen, X.R. (2018). Formation and evolution of oxide inclusions in titanium-stabilized 18Cr stainless steel. *ISIJ Int.* 58 (12), 2280-2287. https://doi.org/10.2355/isijinternational.ISIJINT-2018-332.

Lin, C.K., Pan, Y.C., Frank Su, Y.H., Lin, G.R., Hwang, W.S., Kuo, J.C. (2018). Effects of Mg-Al-O-Mn-S inclusion on the nucleation of acicular ferrite in magnesium-containing low-carbon steel. *Mater. Charact.* 141, 318-327. https://doi.org/10.1016/j.matchar.2018.05.005.

Mitsutaka, H., Kimihisa, I. (2010). *Thermodynamic data for steelmaking*. Tohoku University Press, Sendai, Japan.

Nako, H., Hatano, H., Okazaki, Y., Yamashita, K., Otsu, M. (2014). Crystal orientation relationships between acicular ferrite, oxide, and the austenite matrix. *ISIJ Int*. 54 (7), 1690-1696. https://doi.org/10.2355/isijinternational.54.1690.

Seo, K.Y., Kim, Y.M., Kim, H.J., Lee, C.H. (2015). Characterization of inclusions formed in Ti-containing steel weld metals. *ISIJ Int*. 55 (8), 1730-1738. http://doi.org/10.2355/isijinternational.ISIJINT-2014-800.

Shim, J.H., Cho, Y.W., Chung, S.H., Shim, J.D., Lee, D.N. (1999). Nucleation of intragranular ferrite at $Ti_2O_3$ particle in low carbon steel. *Acta Mater*. 47 (9), 2751-2760. https://doi.org/10.1016/S1359-6454(99)00114-7.

Shim, J.H., Byun, J.S., Cho, Y.W., Oh, Y.J., Shim, J.D., Lee, D.N. (2001). Mn absorption characteristics of $Ti_2O_3$ inclusions in low carbon steels. *Scripta Mater*. 44 (1), 49-54. https://doi.org/10.1016/S1359-6462(00)00560-1.

Takada, A., Komizo, Y.I., Terasaki, H., Yokota, T., Oi, K., Yasuda, K. (2015). Crystallographic analysis for acicular ferrite formation in low carbon steel weld metals. *Welding Int*. 29 (4), 254-261. https://doi.org/10.1080/09507116.2014.921042.

Wang, B.X., Liu, X.H., Wang, G.D. (2018). Inclusion characteristics and acicular ferrite nucleation in Ti-containing weld metals of X80 pipeline steel. *Metall. Mater. Trans. A* 49 (6), 2124-2138. https://doi.org/10.1007/s11661-018-4570-y.

Yamada, T., Terasaki, H., Komizo, Y.I. (2009). Relation between inclusion surface and acicular ferrite in low carbon low alloy steel weld. *ISIJ Int*. 49 (7), 1059-1062. https://doi.org/10.2355/isijinternational.49.1059.

Zhang, T.S., Liu, C.J., Jiang, M.F. (2016). Effect of Mg on behavior and particle size of inclusions in Al-Ti deoxidized molten steels. *Metall. Mater. Trans. B* 47, 2253-2262. https://doi.org/10.1007/s11663-016-0706-x.

Zhang, C.J., Gao, L.N., Zhu, L.G. (2018a). Effect of inclusion size and type on the nucleation of acicular ferrite in high strength ship plate steel. *ISIJ Int*. 58 (5), 965-969. https://doi.org/10.2355/isijinternational.ISIJINT-2017-696.

Zhang, Q.S., Min, Y., Xu, H.S., Liu, C.J. (2018b). Formation and evolution of inclusions in Si-killed resulfurized free-cutting steel. *ISIJ Int.* 58 (7), 1250-1256. https://doi.org/10.2355/isijinternational.ISIJINT-2018-105.

Zou, X.D., Sun, J.C., Zhao, D.P., Matsuura, H., Wang, C. (2018). Effects of Zr addition on evolution behavior of inclusions in EH36 shipbuilding steel: from casting to welding. *J. Iron Steel Res. Int.* 25 (2), 164-172. https://doi.org/10.1007/s42243-018-0022-6.